The Plant Cell, Vol. 15, 694–705, March 2003, www.plantcell.org © 2003 American Society of Plant Biologists

The *DORNRÖSCHEN/ENHANCER OF SHOOT REGENERATION1* Gene of Arabidopsis Acts in the Control of Meristem Cell Fate and Lateral Organ Development

Thomas Kirch,[a] Rüdiger Simon,[a,b] Margit Grünewald,[a] and Wolfgang Werr[a,1]

[a] Institut für Entwicklungsbiologie, Universität zu Köln, Gyrhofstrasse 17, D-50923 Köln, Germany
[b] Institut für Genetik, Heinrich-Heine-Universität Düsseldorf, Universitätstraße 1, D-40225 Düsseldorf, Germany

The two main tasks of a meristem, self-perpetuation and organ initiation, are separated spatially. Slowly dividing cells in the meristem center act as pluripotent stem cells, and only their derivatives in the meristem periphery specify new organs. Meristem integrity and cellular proliferation are controlled in part by regulatory interactions between genes that are expressed in specific subdomains of the meristem. Using transposon-mediated activation tagging, we have identified *Dornröschen* (*drn-D*) mutants of Arabidopsis that prematurely arrest shoot meristem activity with the formation of radialized lateral organs. The mutated gene (*DRN/ESR1*), which encodes an AP2/ERF protein, is expressed in a subdomain of meristem stem cells, in lateral organ anlagen, and transiently in the distal domain of organ primordia. During the development of *drn-D* mutants, expression of the homeobox gene *SHOOTMERISTEMLESS* is downregulated and later reactivated in an altered domain. In addition, we found increased expression of *CLAVATA3* and *WUSCHEL*, two genes that antagonistically regulate stem cell fate in meristems. These findings suggest that the *DRN/ESR1* gene product is involved in the regulation of gene expression patterns in meristems. Furthermore, specific misexpression of *DRN* in meristem stem cells affects organ polarity and outgrowth in the meristem periphery, indicating that *DRN/ESR1* itself, or a process regulated by *DRN/ESR1*, can act non-cell-autonomously. We elaborate on the role of *DRN/ESR1* in meristem and organ development and discuss its possible role in the process of shoot regeneration.

INTRODUCTION

The shoot apical meristem (SAM) is initiated during embryogenesis and subsequently produces the basic elements of the plant shoot structure: leaves and stems. Along the radial axis, the SAM is subdivided into a central zone that harbors a reservoir of pluripotent stem cells and a peripheral zone in which appendages such as leaves and flowers are formed (Bowman and Eshed, 2000; Brand et al., 2001). Leaves originate as small primordia at the meristem flanks; along the radial axis of the primordium, the cells that are closer to the meristem center will form the adaxial (or upper) side of the leaf, and cells that are distal to the meristem center will form the abaxial (or lower) side of the leaf (Bowman et al., 2002). Leaves of *Antirrhinum* seedlings mutant for the *PHANTASTICA* gene are abaxialized and radially symmetric (Waites et al., 1998), indicating that the juxtaposition of adaxial and abaxial domains is required for the lateral and distal outgrowth of the leaf blade.

Several observations indicate an intimate relationship between the establishment of radial axes in the shoot meristem and lateral organs. Mutations in *PINHEAD* (*PNH*) cause an arrest of SAM development after initiation, terminating in a flat meristem accompanied by the formation of abaxialized, radially symmetric organs (Lynn et al., 1999). Expression of *PNH* is found in the vasculature, the SAM, and the adaxial side of leaf primordia, suggesting that these regions may share positional identity. Similarly, abaxial leaf fates are replaced by adaxial fates in the dominant *phabulosa* (*phb*) and *phavoluta* (*phv*) mutants of Arabidopsis (McConnell et al., 2001). The *PHB* and *PHV* genes are members of a small gene family that encodes homeodomain-Leu zipper proteins. *PHB* is expressed in the central region of the SAM and the adaxial domain of leaf primordia. In the gain-of-function *phb-1D* mutant, adaxialized leaves are formed that initiate new meristems all around their bases (McConnell and Barton, 1998). Interestingly, loss-of-function mutations in *PHB* and *PHV* are aphenotypic, indicating that genes of this family may have overlapping or redundant functions. Several genes have been identified in Arabidopsis that promote abaxial identity. *KANADI* (*KAN*) is expressed in the peripheral region of embryos and the abaxial side of leaves (Eshed et al., 2001). When *KAN* was expressed ectopically from a constitutive promoter, the embryos showed peripheral identity even in the central zone. These results suggest that the formation of both radial axes, the adaxial-abaxial axis in leaf primordia and the central-peripheral axis in the SAM, may be controlled by the same mechanism and involve genes that can act in both processes.

During development, cell loss from the meristem attributable to organogenesis in the peripheral zone needs to be balanced by stem cell divisions in the central zone. In Arabidopsis, this balance is maintained by the antagonistic activities of the

[1] To whom correspondence should be addressed. E-mail werr@uni-koeln.de; fax 49-221-470-5164.
Article, publication date, and citation information can be found at www.plantcell.org/cgi/doi/10.1105/tpc.009480.

WUSCHEL (*WUS*) gene (Mayer et al., 1998; Schoof et al., 2000) and the *CLAVATA* (*CLV*) gene (Brand et al., 2000). *WUS*, a homeobox gene, is expressed in a small group of cells underneath the stem cells and inhibits them from differentiating. Stem cells at the meristem tip express the *CLV3* gene, which encodes a secreted protein that activates the CLV1/CLV2 receptor complex, resulting in a restriction of *WUS* expression (Fletcher et al., 1999; Brand et al., 2000). In the absence of *WUS* function (e.g., in *wus* mutant seedlings or when *CLV3* activity is increased), stem cells are lost prematurely from the central zone and SAM development arrests with the formation of radialized organs.

We have used a transposon-based activation tagging system (Tissier et al., 1999) to identify new genes that control shoot meristem development in Arabidopsis. Activation-tagged lines were generated by transposition of a modified *Spm* element, *dSpm-Act*, that carries four copies of the 35S transcriptional enhancer element of *Cauliflower mosaic virus* (CaMV35S). One of the dominant mutants isolated in this screen, *Dornröschen-D* (*drn-D*) (Eckardt et al., 2001), exhibits specific defects in meristem maintenance and lateral organ formation. Cloning of the *DRN* gene revealed that it encodes an AP2/EREB-type transcription factor. Banno et al. (2001) recently identified the same gene as *ENHANCER OF SHOOT REGENERATION1* (*ESR1*), because its misexpression accelerates the regeneration of shoots from cultured root tissue. We report here on the dynamics of *DRN/ESR1* expression during embryogenesis and meristem and organ development. We also analyzed the consequences of *DRN/ESR1* misexpression in plants for gene expression in meristems and propose a role for *DRN/ESR1* in the control of cell fate.

RESULTS

Isolation of the *drn-D* Mutant by Activation Tagging

The early vegetative phase of *drn-D* mutants until the four- to five-leaf stage is unaffected. From leaves 6 to 8 and onward, all leaves appear increasingly radialized, and ~3 weeks after germination, leaf initiation terminates with the formation of filamentous organs that lack the central vasculature (Figures 1A to 1C).

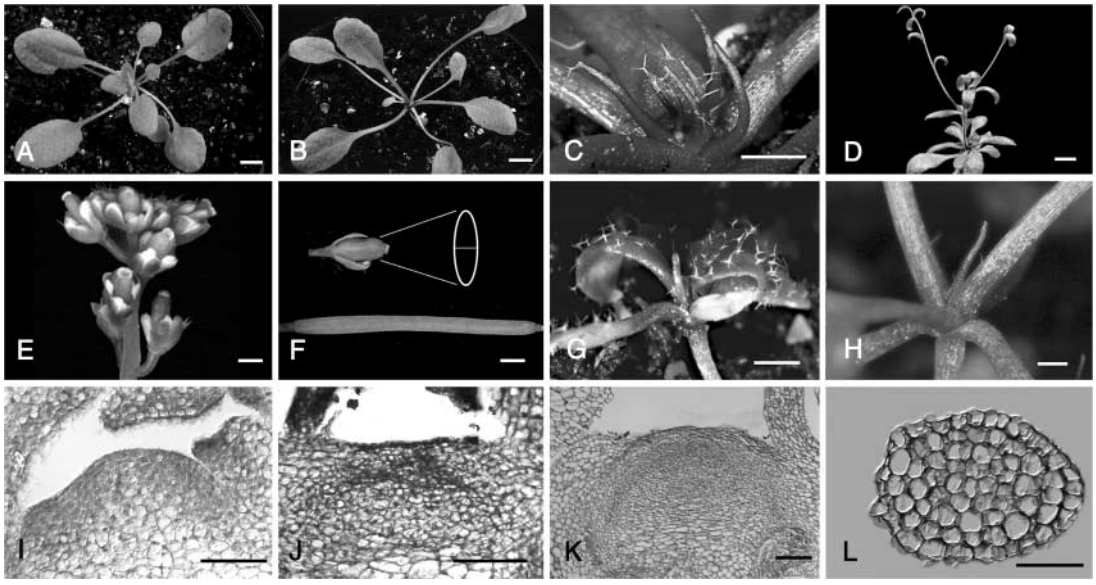

Figure 1. Development of *drn-D* Mutants and Comparison with Transgenic *35S*::*DRN/ESR1* and *35S*::*DRN/ESR1-GR* Plants.

(A) Wild-type Arabidopsis seedling.
(B) *drn-D* mutant seedling at 20 DAG. The shoot meristem has lost activity after the development of seven leaves.
(C) Close-up of the *drn-D* apex in **(B)**. Filamentous organs surround the enlarged meristem.
(D) *drn-D* inflorescence originating from an axillary meristem with a characteristic stop-and-go phenotype. The primary inflorescence meristem arrests, and axillary shoots grow out.
(E) Most *drn-D* plants develop stunted flowers after initiating numerous cauline leaves and several stop-and-go cycles.
(F) Siliques of *drn-D* mutants (top) are shorter and broader than wild-type siliques (bottom).
(G) Phenotype of a class-1 *35S*::*DRN/ESR1* seedling. The SAM is arrested after the development of a single filament.
(H) *35S*::*DRN/ESR1-GR* T2 plant at 7 days after dexamethasone treatment. SAM activity stops after the development of a single radialized organ.
(I) to **(K)** Dellafield staining of longitudinal sections through wild-type **(I)** and *drn-D* shoot meristems at two developmental stages (**[J]** and **[K]**). In the early seedling (6 DAG), the meristem is still active and initiates three to four additional leaves **(J)**, whereas the late (20 DAG) *drn-D* SAM has stopped activity **(K)**. A single filament is sectioned to the right of the apex. Note the size increase in the early and late *drn-D* SAM relative to the wild-type SAM. The characteristic L1, L2, and L3 layering is lost already in the early (6 DAG) seedling, although the SAM remains active.
(L) Dellafield-stained cross-section through a filamentous organ that appears fully radialized.
Bars = 5 mm in **(A)** and **(B)**, 1 mm in **(C)** and **(E)** to **(H)**, 10 mm in **(D)**, and 100 μm in **(I)** to **(L)**.

Approximately 3 months after germination, secondary inflorescence shoots emerge from axillary meristems, which again cease organ formation after the initiation of a few cauline leaves with the formation of radialized lateral organs (Figure 1D). In most *drn-D* plants, inflorescences bearing flowers are formed from axillary meristems after several "stop-and-go" cycles. Floral organ number is normal, but *drn-D* flowers appear stunted and develop short, broad siliques (Figures 1E and 1F).

Compared with the wild type, histological sections show that the *drn-D* SAM is flat and wider in diameter already in the early mutant seedling (Figures 1I and 1J). Meristem size increases further before the SAM finally fails to initiate lateral organs (Figure 1K). Instead of small, meristematic cells, which are typical for the outer cell layers of the wild-type SAM, large and vacuolated cells, indicative of premature cellular differentiation, cover the *drn-D* mutant apex. The filamentous organs that are produced before meristem arrest are radially symmetric (Figure 1L).

Molecular Analysis

As expected for a dominant gain-of-function allele, the *drn-D* phenotype is transmitted to subsequent generations with a 1:1 or 3:1 segregation ratio in backcrosses to the wild type or selfings, respectively. Genomic DNA flanking the *dSpm-Act* transposable element insertion was isolated by inverse PCR and sequenced. The *dSpm-Act* element is located 305 bp 5′ to the ATG translation start codon of *DRN*/*ESR1* (At1g12980; Figure 2A), which encodes a putative AP2/ERF-type transcription factor (Riechmann and Meyerowitz, 1998). On RNA gel blots with total RNA, high *DRN*/*ESR1* transcript levels were detected in *drn-D* mutant seedlings but not in wild-type controls (Figure 2B), indicating that the *drn-D* phenotype was caused by increased transcription of *DRN*/*ESR1*.

Database searches identified a closely related gene, *DRN-like* (At1g24590), that is located 24 centimorgan from *DRN*/*ESR1* on chromosome 1 (Figure 2C). Two adjacent genes, At1g13000 and At1g24570, are conserved flanking both ERFs, suggesting that one of these loci arose via extended intrachromosomal duplication. In a phylogenetic tree based on the conserved AP2 domain, *DRN*/*ESR1* and *DRN-like* are located on one distinct branch, together with five additional *AP2*/*ERF*-type genes (Figure 2D).

Ectopic Expression of *DRN*/*ESR1* in Transgenic Arabidopsis Plants

To confirm that increased expression of *DRN*/*ESR1* causes the *drn-D* phenotype, we expressed the coding region under the control of the *CaMV35S* promoter in transgenic plants. Of 179 primary transformants carrying the transgene, 9 seedlings stopped development after the emergence of two cotyledons (class 1). A second class comprising 22 plantlets was dark green, small, and stunted. After the emergence of three to four tiny leaflets, growth arrested with a single radialized organ (Figure 1G). Sections through seedlings showed an enlarged and disorganized SAM, resembling the meristems of *drn-D* mutant plants (similar to those in Figure 1K). A third class of transgenic plants (18 of 179) was characterized by strong dwarfism, epinastic leaves, delayed bolting, and short but broad siliques. The majority of transgenic plants (130 of 179; class 4), were mildly dwarfed but formed short and broad siliques. Plants of all four phenotypic classes showed at least some of the phenotypic alterations that we observed in *drn-D* mutants: alterations in silique shape (classes 3 and 4), growth retardation (classes 2, 3, and 4), and meristem arrest (classes 1 and 2). RNA gel blot analysis confirmed that differences between phenotypic classes were attributable to differences in the level of transgene expression (data not shown). Loss of SAM activity and radialization of leaves were detected only in plants that expressed the transgene at high levels.

To control ectopic *DRN*/*ESR1* gene activity, we expressed a fusion protein of *DRN*/*ESR1* and the hormone binding domain of the rat glucocorticoid receptor (*GR*) in Arabidopsis (Lloyd et al., 1994). The development of transgenic plants (T1) expressing the *DRN*/*ESR1*-*GR* fusion from the *CaMV35S* promoter appeared normal. Application of dexamethasone to 30 individual lines of the T2 progeny at the two-leaf stage resulted in SAM arrest within 1 week, after the development of three to four additional leaflets (Figure 1H). In most cases, SAM activity terminated with the initiation of radialized organs, as in *drn-D* mutant plants.

In summary, we have shown that misexpression of *DRN*/*ESR1* is responsible for the severe meristem defects in *drn-D* mutants. In addition, *DRN*/*ESR1* activity requires access of the protein to the nuclear compartment, supporting a role in transcriptional control.

Expression Pattern of *DRN*/*ESR1* during Development

We used RNA in situ hybridizations and a *β-glucuronidase* (*GUS*) reporter gene for expression analysis of *DRN*/*ESR1*. To construct the *GUS* reporter, the *DRN*/*ESR1* coding region was replaced by the *GUS* open reading frame in a genomic clone carrying 4.8-kb DNA sequences upstream of the ATG and 1.5-kb DNA sequences downstream of the termination codon. GUS staining patterns were comparable to those revealed by RNA in situ hybridization.

During embryogenesis, expression was detected first in the proembryo at the four-cell stage (Figure 3A) and throughout the embryo at the globular stage. At the early heart stage, transcripts accumulated at high levels in the emerging cotyledons and at lower levels at the position of the prospective SAM (Figure 3B). Expression in cotyledons was only transient, and from the torpedo stage onward, transcripts were found exclusively in the L1 layer of the SAM (Figure 3C). When the seedling had germinated, expression was found in young leaf primordia (Figure 3D) and in the two outer cell layers, L1 and L2, of the SAM. After floral induction, RNA was detected in the central zone of the inflorescence meristem and in the flower primordia P_{-1}, P_0, and P_2 (Figures 3E to 3L). Expression extended from the center of the SAM into the P_{-1} primordium (Figures 3F to 3H) and was found in the P_0 and P_2 positions. In the P_2 primordium, high levels of RNA were confined to the apical region of the primordium (cf. Figures 3I, 3J, and 3K with 3L). Interestingly, we failed to detect RNA at the P_1 position. During floral development,

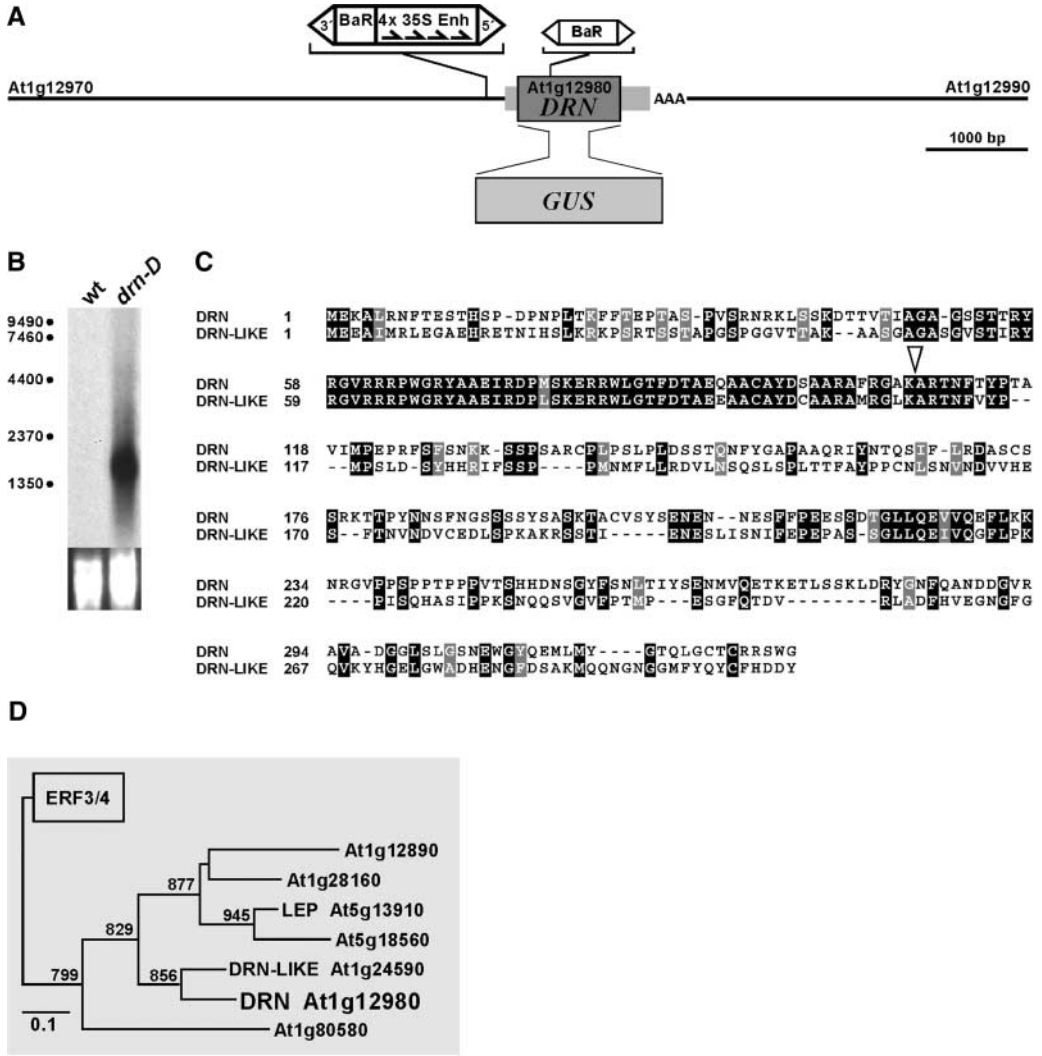

Figure 2. Structure of the *drn-D* Allele and Phylogeny.

(A) Position and orientation of the activating *en/En* transposable element insertion in *drn-D* relative to the *DRN/ESR1* transcription unit and the neighboring At1g12970 and At1g12990 genes. The *CaMV35S* enhancer elements direct towards the *DRN/ESR1* coding region. In the loss-of-function *drn-1* allele, a modified *dSpm* element is inserted into the coding region. The 5′ and 3′ untranslated regions are shown as gray boxes. In the *DRN/ESR1-GUS* reporter construct, the *DRN/ESR1* coding region was replaced by the *GUS* coding region.

(B) RNA gel blot with 10 μg of total RNA from wild-type (wt) and *drn-D* seedlings probed for *DRN/ESR1* expression. *DRN/ESR1* is expressed at high levels in *drn-D* mutant seedlings. Failure to detect *DRN/ESR1* RNA in the wild type is attributable to the very restricted expression domain in the SAM and early primordia anlagen.

(C) DRN/ESR1 protein sequence compared with the sequence of its closest relative, *DRN-like* (At1g24590). The highly conserved AP2 domain starts at position 56 and ends at residue 116. Within the 68–amino acid AP2 domain, 58 residues are conserved, and a scaffold of Pro (7) and Ser/Thr (11) residues is shared in the C-terminal region. Identical residues are highlighted in black, and isomorphic replacements are highlighted in gray. The open triangle at position 107 indicates the insertion of the *dSpm* element into the AP2 domain in the *drn-1* allele.

(D) DRN/ESR1 is located on a distinct phylogenetic branch of the AP2/ERF transcription factor family. Only one other protein of this family, LEAFY PETIOLE (LEP; van der Graaff et al., 2000), has been analyzed to date.

expression always was found in three to four cell layers in the center of floral meristems (Figures 3E to 3H) and in the anlagen of sepals and stamens (Figure 3L). *DRN/ESR1* transcripts were found in single L1 layer cells marking ovule anlagen at staggered positions of the two placentae (Schneitz et al., 1995), and expression persisted in a single apical cell during further development of the ovule primordia (Figures 3M and 3N).

To confirm RNA expression in the central zone of meristems, we introduced the *DRN/ESR1-GUS* reporter line into *clv3-2* mutants, which accumulate stem cells in the meristem center.

GUS activity was found in an enlarged domain, consistent with the expression of *DRN*/*ESR1* in the stem cell domain (Figure 3P).

In summary, *DRN*/*ESR1* was expressed from embryogenesis onward in the central zone of the shoot apical and floral meristems, in organ anlagen, and (transiently) in the distal domains of organ primordia.

SAM Organization in the *drn-D* Mutant

Arrest of meristem activity in *drn-D* mutants could be caused by changes in the activity or expression levels of genes that are required for meristem function. For example, an active shoot meristem was not maintained in *shootmeristemless* (*stm*) and *wus* mutants or when *CLV3* was expressed at increased levels. To characterize the changes in the size and organization of *drn-D* meristems, we analyzed the expression patterns of *DRN*/*ESR1*, *STM*, *CLV3*, and *WUS* in *drn-D* mutant seedlings by RNA in situ hybridization.

DRN/*ESR1*

In the wild type, *DRN*/*ESR1* was expressed in the L1 and L2 layers of the central zone and in young organ primordia. Meristems of *drn-D* mutant seedlings at 7 days after germination (DAG) expressed *DRN*/*ESR1* in an enlarged domain that extended into the differentiated stem tissue underneath (Figure 4A). In the inactive SAM at 20 DAG, expression was restricted to the deeper regions of the enlarged apex (Figure 4B). The insertion of CaMV enhancer elements upstream of the *drn-D* transcription unit thus resulted in an enlarged expression domain but not in general ectopic expression throughout the plant.

WUS

Previous studies have shown that *WUS* promotes both stem cell fate and *CLV3* expression. In the wild type, *WUS* was expressed in the organizing center, a small group of cells underneath the stem cell zone of shoot and floral meristems (Mayer et al., 1998). In the inactive meristem of *drn-D* mutant seedlings, we found *WUS* RNA in an enlarged basal region, which largely overlaps with the late *DRN*/*ESR1* pattern (Figure 4C).

CLV3

In the wild type, *CLV3* is expressed only in the putative stem cells in the central zone of shoot and floral meristems (Fletcher et al., 1999). Although a small increase in the size of the *CLV3* expression domain was detectable in early *drn-D* seedlings (data not shown), it still was confined to the apical tip of the SAM. Later in development, *CLV3* expression was shifted into a deeper region of the mutant seedling meristem, where it was coexpressed with *DRN*/*ESR1* and *WUS* (Figure 4D).

STM

The *STM* gene was expressed in all cell layers of the wild-type SAM but was lacking in cells that were recruited into lateral organ primordia at the flanks of the meristem (Long et al., 1996) (Figure 4E). In *drn-D* seedlings at 6 DAG, *STM* expression was comparable to that in the wild type (Figure 4F). However, we failed to detect any expression of *STM* in *drn-D* seedlings at 8 to 10 DAG (Figure 4G). In the arrested apex (20 DAG), *STM* expression was restored in an inverted cup–shaped domain consisting of small and potentially meristematic cells (Figure 4H). Although *DRN*/*ESR1* and *STM* were expressed in overlapping domains in early *drn-D* seedlings, both patterns appeared mutually exclusive in the inactive apex.

In summary, we observed a drastic reorganization of gene expression domains and of the structure of *drn-D* shoot meristems. During seedling development, *DRN*/*ESR1* expression expanded from an initially small group of cells at the meristem tip into deeper regions; a similar change of gene expression was found for *CLV3* and *WUS*. Furthermore, *STM* expression was first lost in the meristem but then reactivated in a novel pattern in the deeper meristem region. At the same time, new layers of apparently differentiated cells were formed at the apex that failed to express *STM*.

DRN/*ESR1* Acts Independently of *STM*, *WUS*, and *CLV*

To determine if the inactivity of *drn-D* meristems is caused by misexpression of *STM*, *WUS*, or *CLV3*, we created double mutants of *drn-D* with *stm*, *wus*, and *clv3*.

wus drn-D

The SAM of *wus-1* mutants appeared flat and arrested after the formation of the first leaves (Figure 4I); new leaf primordia and secondary meristems were initiated from the leaf axils. *wus drn-D* seedlings displayed a more extreme phenotype: the first two leaves were converted to radialized filaments, and no secondary meristems were formed (Figure 4J). Thus, ectopic expression of *DRN*/*ESR1* abolished residual SAM activity that was maintained in the absence of *WUS* function.

clv drn-D

Increased activity of the *CLV* pathway (e.g., increased expression of *CLV3*) results in the downregulation of *WUS* and stem cell loss (Brand et al., 2000). To determine whether the arrest of meristem activity in the *drn-D* mutant is mediated by increased *CLV* signaling, we created double mutants of *drn-D* with the loss-of-function mutant *clv3-2*. We observed an additional increase in meristem size and a subsequent arrest of meristem function, comparable to the effects of *drn-D* in a wild-type background. Inflorescences that formed during later development initiated radially symmetric filaments and flowers with an increased number of floral organs. In most *clv* mutants, floral meristems were not consumed entirely by the formation of carpels from the meristem center. Ectopic *DRN*/*ESR1* expression further enhanced this phenotype: in *clv3-2 drn-D* mutants, disorganized tissue grew out from the center of floral meristems, indicating that *DRN*/*ESR1* can promote cell proliferation in the meristem center (Figure 4K).

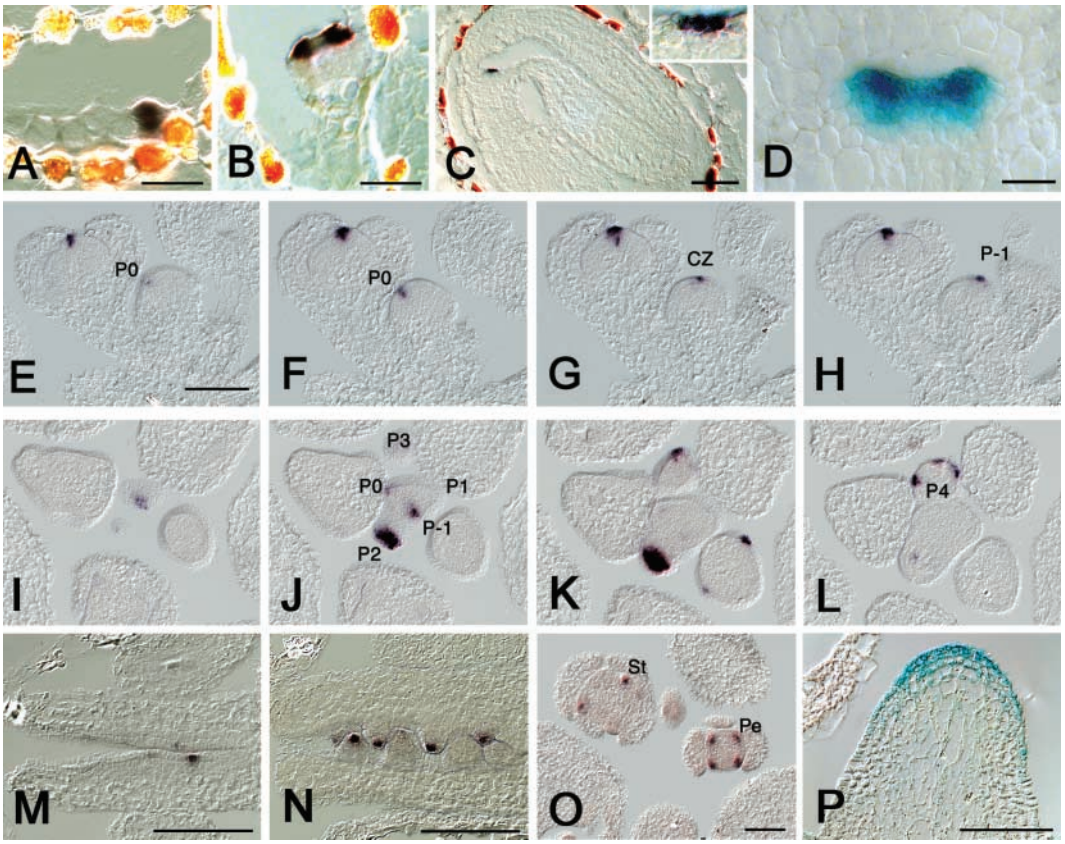

Figure 3. *DRN/ESR1* Expression Pattern.

(A) Early embryo. *DRN/ESR1* transcripts are confined to the four-cell embryo proper.
(B) At the heart stage, *DRN/ESR1* is expressed in the emerging cotyledons and at low levels where the SAM will be formed.
(C) Longitudinal section through a walking-stick stage embryo. *DRN/ESR1* transcripts are restricted to the SAM.
(D) Whole mount of a *DRN/ESR1-GUS* seedling at 4 DAG showing high *GUS* activity in both leaf primordia and weak expression in the SAM.
(E) to **(H)** Serial longitudinal sections through inflorescence and floral meristems. The *DRN/ESR1* expression domain extends from the P_0 primordium (**[E]** and **[F]**) through the central zone **(G)** into the P_{-1} primordium **(H)**. In a stage-4 flower (**[E]** to **[H]**, at left), *DRN/ESR1* is expressed in the central zone.
(I) to **(L)** Transverse sections through the inflorescence. *DRN/ESR1* activity extends from the center (**[I]** and **[J]**) into the P_{-1} primordium **(I)**. In the section below, *DRN/ESR1* activity is high in P_{-1} at the periphery of the inflorescence meristem but weaker toward the center **(J)**, which is consistent with the superficial expression pattern seen in the longitudinal sections. In the same section **(J)**, strong expression is seen in the P_2 primordium, but no transcripts are found in P_1. The signal in P_0 already is disappearing. *DRN/ESR1* transcripts are restricted to the apical half of the P_2 primordium (**[J]** to **[L]**). **(K)** and **(L)** show expression in the sepals of a P_4 floral meristem.
(M) and **(N)** Sections through placental tissue in the developing gynoecium. *DRN/ESR1* is expressed in the interdigitating ovule anlagen of a stage-7 flower **(M)** and in the most apical cell of emerging ovule primordia at later stages **(N)**.
(O) Cross-section through flowers showing the expression of *DRN-like* in petals and stamens.
(P) *clv3-2* mutant inflorescence. The *DRN/ESR1-GUS* marker is expressed in the expanded stem cell domain at the inflorescence tip.
CZ, central zone; P_{-1} to P_4, primordia; Pe, petal; St, stamen. Bars = 10 μm in **(A)**, **(B)**, and **(D)** and 50 μm in all other panels.

stm drn-D

Loss-of-function mutations in *STM* result in a failure to initiate a shoot meristem during embryogenesis. In strong *stm-5* mutants, secondary meristems that arise at the base of the cotyledons may form leaves with axillary meristems, resulting in a seedling that consists of a disorganized leaf rosette (Endrizzi et al., 1996). In *stm-5 drn-D* double mutants, these secondary meristems initiated four to six leaves; some of these were at least partly radialized, and leaf initiation stopped with the formation of small, filamentous organs (Figure 4L). Thus, the defect in meristem maintenance that is characteristic of *stm* mutants was enhanced by *DRN/ESR1* upregulation.

Misexpression of *DRN/ESR1* in *drn-D* affected meristem

function and lateral organ development in all double mutant combinations, indicating that *DRN*/*ESR1* can act independently of *STM*, *WUS*, and *CLV3*.

A Loss-of-Function Allele Is Aphenotypic

The *Dornröschen* phenotype reflects the consequences of ectopic or increased gene expression. We isolated a loss-of-function allele, *drn-1*, from the *SLAT* collection (Tissier et al., 1999) carrying a single *dSpm* transposable element inserted in the coding region (Figure 2C). The *dSpm* insertion disrupts the conserved RAYD element in the AP2 domain (Riechmann and Meyerowitz, 1998); therefore, the insertion allele is likely to be a null allele. To date, we were unable to detect any phenotypic alteration in plants homozygous for the potential null allele compared with the wild type.

A candidate gene that may act redundantly with *DRN*/*ESR1* is *DRN-like* (At1g24590), which shows the highest sequence similarity. *DRN-like* was expressed in organ anlagen in a similar pattern to *DRN*/*ESR1* (Figure 3O) but not in the stem cell domain of meristems. Like *CaMV35S-DRN*/*ESR1* transgenic plants, plants that expressed *DRN-like* from the CaMV35S promoter exhibited dwarfism or alterations in silique shape but maintained a functional shoot meristem during development (data not shown). Thus, *DRN*/*ESR1* and *DRN-like* may have only partially overlapping functions, because both expression in the central zone and shoot meristem arrest in overexpression lines were specific for *DRN*/*ESR1*.

Expression of *DRN*/*ESR1* in the Central Zone Affects Organ Development in the Periphery

Our previous experiments had shown that misexpression of *DRN*/*ESR1* affects both meristem maintenance and the development of organs in the meristem periphery. Here, we used the *CLV3* promoter to misexpress *DRN*/*ESR1* only in the central zone of meristems. At 10 DAG, all transgenic T1 plants (n = 154) had formed two to four normal leaves (Figure 5A). In 60% of the plants (class 1, n = 92), the apical dome enlarged progressively, which was accompanied by the initiation of a few radialized organs. Later organ primordia (18 DAG) remained reduced to small protrusions (Figure 5B). Scanning electron microscopy revealed that the shoot meristem, resting on a ball-shaped shoot axis, still was able to initiate organ primordia in a spiral phyllotaxis. However, during displacement to the periphery, these organs failed to grow out and were overgrown by the massively enlarging shoot axis (Figures 5C and 5D). We were unable to detect a functional meristem at 25 DAG. Class-2 transgenic plants (25%, n = 38) developed initially like class-1 plants, but the highly enlarged shoot axis bolted after evocation, and floral primordia were initiated (Figure 5E) that produced viable seeds. The remaining transgenic plants (class 3, n = 24) developed normally during the vegetative phase. After bolting, cauline leaves were replaced by filamentous organs (Figure 5F). Transmission of the phenotype to the subsequent generation was confirmed in 32 lines that produced seeds. The recovery of strong class-1 phenotypes among T2 progeny of class-2 and -3 primary transformants indicates that heterozygosity and homozygosity (i.e., differences in transgene expression levels) could account for the phenotypic differences.

Thus, the expression of *DRN*/*ESR1* in the central zone of meristems is sufficient to affect organ development in the peripheral zone, indicating that *DRN*/*ESR1* can act non-cell-autonomously.

DISCUSSION

Role of *DRN*/*ESR1* in Gene Regulation in the Meristem

We have shown that ectopic expression of *DRN*/*ESR1* throughout the plant, and also misexpression from the *CLV3* promoter in the central zone where *DRN*/*ESR1* is expressed normally, have dramatic consequences for meristem and organ development. The SAM arrests the formation of lateral organs with the initiation of radialized leaves. One simple explanation for the failure to maintain a functional meristem could be that cells in the meristem stop dividing. However, compared with the wild-type SAM, the shoot apex of *drn-D* mutants was enlarged massively, with several layers of large and differentiated cells at the tip. This finding suggests that cells in *drn-D* meristems still divide but are unable to maintain their appropriate identity. At ~21 DAG, several new layers of apparently differentiating cells were found at the apex of *drn-D* seedlings that did not express any of the meristem markers we tested (*CLV3*, *STM*, and *WUS*). This proliferation and differentiation of cells at the meristem tip could indicate that *DRN*/*ESR1* acts by promoting cell division and ultimately cellular differentiation. Alternatively, the structural changes in *drn-D* meristems and the defects in organ formation could be caused by the misregulation of genes that are crucial for meristem function.

One of the potential target genes for regulation by *DRN*/*ESR1* is *STM*. In young *drn-D* meristems, *STM* was downregulated when *DRN*/*ESR1* expression increased. At later stages, *STM* expression was reactivated in a narrow region of cells, forming an inverted cup–shaped domain. *DRN*/*ESR1* and *STM* RNAs then were found in adjacent, nonoverlapping domains (a similar relationship between *STM* and *DRN*/*ESR1* expression was found in wild-type organ primordia that express only *DRN*/*ESR1* but not *STM*). Thus, cellular differentiation at the apex of *drn-D* meristems may result from the loss of *STM* expression at the meristem apex, indicating that *DRN*/*ESR1* can repress *STM* expression. Alternatively, increased expression of *DRN*/*ESR1* may promote cell differentiation, resulting in an indirect downregulation of *STM* expression at the meristem tip.

As described in Introduction, the mutual regulation of *CLV3* and *WUS* is required to maintain an appropriate pool of stem cells in meristems. We found that in addition to *STM*, the expression patterns of *CLV3* and *WUS* also were altered in *drn-D* mutants. In wild-type meristems, *CLV3* was expressed in stem cells and *WUS* was expressed in a separate, subjacent domain. In *drn-D* mutants, the expression domains of both genes increased in size and shifted to a basal region, where *DRN*/*ESR1*, *CLV3*, and *WUS* were coexpressed. Given that *CLV3* and *DRN*/*ESR1* were coexpressed in the stem cell zone of wild-type meristems, one role of *DRN*/*ESR1* may be to promote *CLV3* expression. Consistent with this idea, we found that *CLV3*

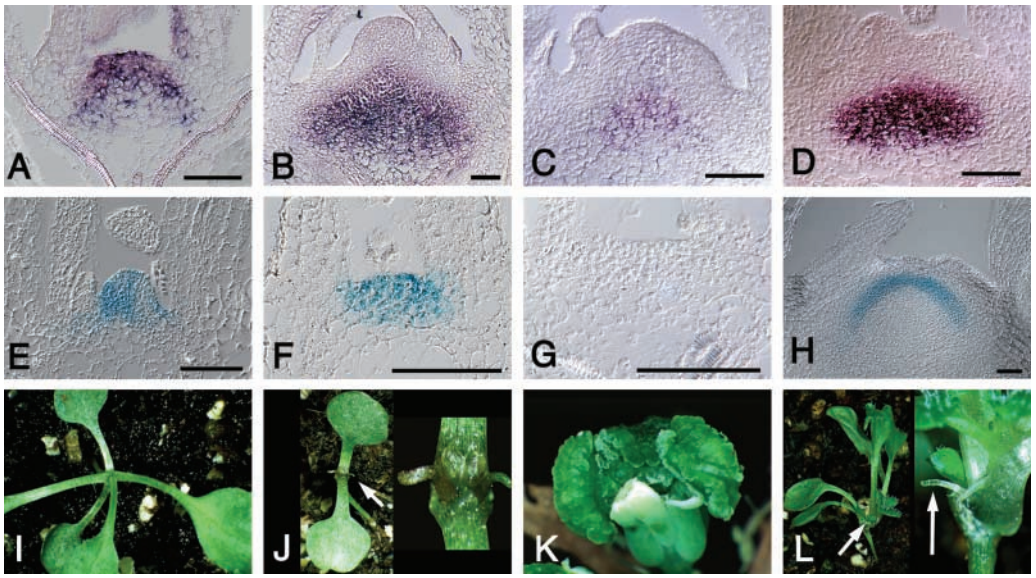

Figure 4. Gene Expression Patterns in *drn-D* Mutants and Double Mutant Analysis.

Expression of *DRN/ESR1*, *WUS*, and *CLV3* in the shoot meristem of *drn-D* mutants was analyzed by RNA in situ hybridization. *STM* patterns were detected using a *STM*::*GUS* reporter line.

(A) *DRN/ESR1* expression in *drn-D* seedlings at 7 DAG.

(B) At 20 DAG, the *DRN/ESR1* expression domain has shifted to a central position in the meristem.

(C) and **(D)** Both *WUS* **(C)** and *CLV3* **(D)** are expressed in an expanded domain in *drn-D* mutants at 20 DAG.

(E) to **(H)** *STM* expression patterns were analyzed using a *STM*::*GUS* reporter. Compared with that in the wild type **(E)**, the *STM* pattern remains normal in *drn-D* seedlings at 6 DAG **(F)**, although the SAM has already lost its dome shape. At 10 DAG **(G)**, *STM* is no longer expressed. In arrested meristems at 20 DAG **(H)**, *STM* is reexpressed in an inverted cup–shaped domain. Note that *DRN/ESR1*, *WUS*, and *CLV3* all are expressed in a common central domain of the SAM at 20 DAG, whereas *STM* is expressed in overlying cells (cf. **[B]** with **[D]** and **[H]**).

(I) to **(L)** Analysis of double mutant combinations with *drn-D*.

(I) *wus-1* seedling with three fully developed leaves. The shoot meristem has terminated organ initiation.

(J) *wus-1 drn-D* double mutant. The first two leaf primordia are radialized (arrow) and the SAM has lost activity.

(K) Callus-like tissue proliferates from the center of a *clv3-2 drn-D* flower.

(L) *stm-5 drn-D* double mutant with a lateral shoot (arrow) emerging from the hypocotyl after the formation of a few leaves. The arrow in the close-up at right shows a filamentous organ that developed when the axillary meristem arrested.

Bars = 50 μm.

expression levels increased in *drn-D* mutants even before gross changes in meristem structure became apparent (data not shown). However, it is puzzling that increased expression of *CLV3* in *drn-D* mutants did not result in the expected downregulation of *WUS* (Brand et al., 2000). This finding may be explained if increased *DRN/ESR1* expression interferes with or abolishes signaling via the *CLV* pathway. Alternatively, *DRN/ESR1* could promote the expression of both *CLV3* and *WUS* in the meristem. However, *DRN/ESR1* misexpression affected shoot development in all mutant backgrounds analyzed to date, indicating that *DRN/ESR1* may not act exclusively by regulating *STM*, *WUS*, or *CLV3* expression.

To date, the data have shown that *DRN/ESR1*, which encodes an AP2/ERF-type transcription factor, can regulate the expression patterns of *STM*, *CLV3*, and *WUS* in the SAM. In addition, we found that increased *DRN/ESR1* expression not only interfered with the maintenance of an active meristem but also affected leaf polarity. These organ polarity defects could be caused by increased *DRN/ESR1* expression within leaf primordia, resulting in the misregulation of genes that control the establishment of adaxial or abaxial leaf domains. However, radialized organs that failed to grow out also were formed in *CLV3-DRN/ESR1* transgenic plants, in which the misexpression of *DRN/ESR1* was confined to the central zone of meristems. The establishment of dorsoventral polarity in lateral organs requires the generation and perception of positional information along the radius of the meristem, and several Arabidopsis mutants that fail to establish or maintain a SAM terminate development with the formation of radially symmetric leaves (Lynn et al., 1999; McConnell et al., 2001). Thus, the formation of filamentous organs in *drn-D* may result from the dramatic changes in meristem structure and gene expression patterns, interfering with the acquisition of dorsoventral polarity in leaf founder cells.

Does *DRN/ESR1* Act in a Signaling Pathway That Controls Cell Proliferation?

Although the SAM of *drn-D* mutants arrests organ formation comparable to *stm* or *wus* mutants, it is surprising that the meristem continues to grow. Notably, we found that meristem size also increased when *DRN/ESR1* was expressed only in the central zone of the meristem, indicating that *DRN/ESR1* may act non-cell-autonomously to promote tissue growth in the meristem periphery. For example, *DRN/ESR1* could be involved in the generation or perception of signals that promote cell division, such as cytokinins.

In tissue culture experiments, the regeneration of shoots from root cultures requires a balanced supply of auxins and cytokinins. Transient overexpression of *DRN/ESR1* in Arabidopsis root explants was shown recently to permit shoot regeneration even in the absence of exogenous cytokinin (Banno et al., 2001). In the presence of cytokinin, *DRN/ESR1* overexpression increased the overall efficiency of shoot regeneration; these experiments suggested that *DRN/ESR1* may act synergistically with cytokinins. Furthermore, the authors reported on the cytokinin inducibility of *ESR1* expression in roots after pretreatment with auxin analogs, concluding that *DRN/ESR1* regulates the induction of shoot regeneration after the acquisition of competence for organogenesis.

Is there a similar interdependence between *DRN/ESR1* activity and phytohormones during normal development? Although Banno et al. (2001) reported that *DRN/ESR1* expression can be induced in root cultures, we did not detect *DRN/ESR1* expression in roots of wild-type Arabidopsis seedlings. Because cytokinins are present throughout plant meristems and organs (Jacqmard et al., 2002), we regard it as unlikely that the complex and cell type–specific expression pattern of *DRN* is controlled mainly by cytokinin levels. Furthermore, we also showed that increased *DRN/ESR1* expression represses *STM* in the meristem, whereas increased cytokinin signaling promotes the expression of *STM* and other homeobox genes (Rupp et al., 1999). It may be premature to speculate on a direct connection between DRN/ESR1 and cytokinin signaling. From our analysis, we propose that enhanced shoot regeneration from *DRN/ESR1*-expressing roots is caused by the activation of genes that promote meristem formation and activity.

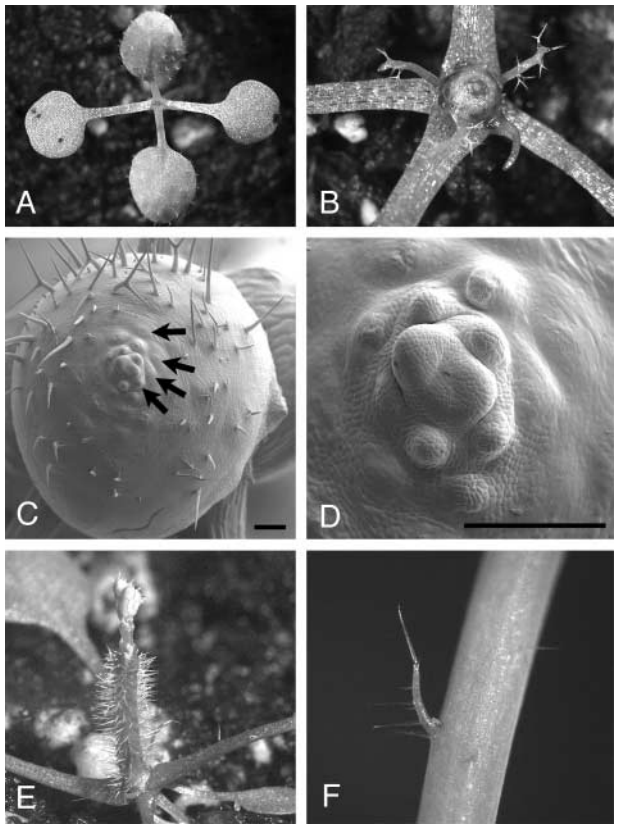

Figure 5. *DRN/ESR1* Misexpression in the Central Zone Arrests Meristem Activity and Affects Organ Development in the Periphery.

Transgenic plants expressing *DRN/ESR1* from the *CLV3* promoter.
(A) Class-1 *CLV3-DRN/ESR1* seedling at 10 DAG. Two normal leaves have developed.
(B) At 18 DAG, the expanded shoot apex is surrounded by radialized organs.
(C) and **(D)** Scanning electron micrographs reveal that organs are initiated but fail to grow out during later stages (arrows).
(E) Inflorescence of a class-2 seedling.
(F) Radialized cauline leaf formed on the inflorescence of a class-3 seedling.
Bars = 100 μm.

Control and Consequences of *DRN/ESR1* Expression

The expression pattern of *DRN/ESR1* mRNA is very dynamic. *DRN/ESR1* is expressed first at the four-cell stage of embryogenesis. From a ubiquitous distribution in the globular embryo, the expression domain focuses on the emerging cotyledons during the heart stage. Toward the end of embryogenesis and at later stages in the vegetative, inflorescence, and floral meristems, *DRN/ESR1* transcripts are found consistently at the apical tip of shoot and floral meristems, where expression is confined to the central zone. Furthermore, *DRN/ESR1* is expressed in the anlagen of lateral organs, where expression is maintained for a short period at the tip of the primordium. For example, *DRN/ESR1* is expressed in single epidermal cells of the ovule anlagen and remains expressed in the most apical cell of the growing ovule.

What are the candidate genes that may specify the *DRN/ESR1* expression pattern? Two observations indicate that *DRN/ESR1* expression in the meristem center may be regulated by *WUS* activity, comparable to the control of *CLV3* expression. First, both *CLV3* and *DRN/ESR1* mRNAs are found only in the putative stem cells at the meristem tip. Second, in *clv* mutant meristems that accumulate stems cells as a result of unrestricted *WUS* expression, both *CLV3* (Fletcher et al., 1999) and *DRN/ESR1* (Figure 3P) are expressed in an expanded domain. The expression pattern of *DRN/ESR1* in the meristem center and in organ anlagen resembles the distribution of *PHB* mRNA (McConnell et al., 2001), indicating that *PHB* may regulate some aspects of *DRN/ESR1* expression or vice versa or that both genes interpret the same positional information.

There is a common theme in the spatial distribution of *DRN/ESR1* mRNA: in all meristems and organs, *DRN/ESR1* expression becomes confined to apical regions. However, the tips of lateral organs are the first to cease cell division and start differentiation, whereas meristem tips are the source of nondifferentiating stem cells. Increased *DRN/ESR1* expression in the *drn-D* mutant results in cellular differentiation at the meristem tip, suggesting that *DRN/ESR1* plays a role in repressing stem cell fate. In wild-type meristems, *DRN/ESR1* could counteract the *WUS*-dependent stem cell–promoting signal and foster the exit from stem cell fate in the immediate descendants of stem cells. *DRN/ESR1* activity during the early stages of organ development then has to be antagonized by other proteins, allowing *DRN/ESR1* to promote cell differentiation only at later stages.

To date, we have not been able to associate a loss-of-function phenotype with *DRN/ESR1*. Several genes that are related closely to *DRN/ESR1* may be redundant to one another, and multiple mutations could be required to obtain a phenotype. Consequently, the *drn-D* gain-of-function allele provided a unique resource to determine the role of *DRN/ESR1* in shoot meristem development. Notably, our double mutant analysis indicates that ectopic *DRN/ESR1* activity can act independently of *STM*, *WUS*, and *CLV3* functions; thus, DRN/ESR1 may be a redundant component of a new signaling pathway in the Arabidopsis SAM.

METHODS

Growth Conditions

Arabidopsis thaliana plants were grown on soil or 0.5 × Murashige and Skoog (1962) medium supplemented with 1% Suc under either a 10-h-light/14-h-dark regime (short-day conditions) at 18°C or a 16-h-light/8-h-dark regime (long-day conditions) at 22°C.

Genetics

Details of the TAMARA transposable element activation tagging system are available upon request. The *drn-D* mutant line identified in the TAMARA population carried a single *dSpm/En* transposon insertion in the Columbia background. For the generation of double mutant lines, the genetic background of *drn-D* was homogenized with the Landsberg *erecta* background of *stm-5*, *wus-1*, *clv1-4*, *clv2-1*, and *clv3-2* for a least three generations by the selection of seedlings with Columbia characteristics among BASTA-resistant progeny. The transmission of the *drn-D* allele in various mutant backgrounds was followed by use of the BASTA resistance marker in the enhancing *dSpm-Act* element. All phenotypes were analyzed among BASTA-resistant F2 progeny.

Chimeric Constructs and Plant Transformation

The *DRN/ESR1* (At1g12980) and *DRN-like* (At1g24590) coding sequences were amplified from genomic DNA by PCR with the primers 5′-ACCAACCATGGAAAAAGCCTTGAGAAAC-3′ and 5′-ACCAAAACTCAAAACATAATC-3′ (for *DRN/ESR1*) or 5′-GGTCAACCATGGAAGAAGCAATCA-3′ and 5′-GATAAGCACGTAAAAAGTAGAACA-3′ (for *DRN-like*). After subcloning into the vector pCRII-TOPO (Invitrogen, Carlsbad, CA), the open reading frame was cloned directionally behind the *CaMV35S* promoter into the vector pRTΩNOT/AscI; in a second step, it was transferred to a pGPTV binary vector using the AscI sites flanking the expression cassette (Überlacker and Werr, 1996).

For *CaMV35S-DRN/ESR1-GR*, the *DRN/ESR1* open reading frame was inserted as a BamHI-XbaI fragment into the binary vector pBI-ΔGR (Lloyd et al., 1994) in frame with the hormone binding domain of the glucocorticoid receptor at the C terminus after amplifying the At1g24590 open reading frame with the primers 5′-ACCAACCATGGAAAAAGCCTTGAGAAAC-3′ (forward) and 5′-GGATCCCACGATCTTCGGCAAG-3′ (reverse) and subcloning as described above.

For the *DRN/ESR1* promoter–*β-glucuronidase* (*GUS*) fusion, a 4.8-kb DNA sequence upstream from the *DRN/ESR1* translation start and 1.5 kb downstream of the translational stop codon were amplified by PCR (Expand-Polymerase; Roche, Mannheim, Germany) using BAC F13K23 (Resource Centre, Berlin, Germany) as a template with the following primers: 5′-TTTGGTTCCTAGGGTTTTGGTTTG-3′, 5′-CGTTTGTTCATCTTTCGTTTCAGC-3′, 5′-GGAGAGCTCGATATTCATCATGATTATG-3′, and 5′-AGCTTGGAGCTCGAATAGAGTTCAAC-3′. The 5′ and 3′ fragments were inserted upstream and downstream, respectively, of the *GUS* coding region in pGPTV-BAR (Becker et al., 1992).

For *CLV3-DRN/ESR1*, the *DRN/ESR1* coding region was inserted between the 1.5-kb *CLV3* upstream promoter and the 1.2-kb downstream enhancer sequences. For details of the construct, see Brand et al. (2002). For *STM-GUS*, 5.5 kb of the *STM* gene 5′ to the putative transcription start site were fused to the *GUS* gene in binary vector pGPTV. Transgenic plants were generated by vacuum infiltration of Arabidopsis ecotype Columbia recipient plants using *Agrobacterium tumefaciens* strain GV3101 (Bechtold and Pelletier, 1998). Transgenic plants were selected using resistance against the herbicides kanamycin and BASTA.

RNA Gel Blot Analysis and in Situ Hybridization

Total RNA was extracted from 3-week-old seedlings (Chomczynski and Sacchi, 1987), separated on a 1.2% formaldehyde gel, and transferred onto Hybond N^+. Hybridization was performed according to standard protocols with a 670-bp DNA probe extending from an internal PvuII site 3′ of the AP2 domain to the translational stop codon, which was labeled by nick translation with α-^{32}P-dCTP (Amersham). Nonradioactive in situ hybridization experiments were performed essentially as described previously (Bradley et al., 1993).

PCR Conditions and Primers

The position of the *dSpm-Act* element in the Arabidopsis genome was determined by inverse PCR. Genomic DNA (0.2 to 0.5 μg) was digested with Sau3AI or RsaI and precipitated after phenol/chloroform extraction. Autoligation was performed overnight at 16°C in a total volume of 300 μL with 5 units of T4 DNA ligase and stopped by phenol/chloroform extraction before PCR amplification. PCR conditions were as follows: 5 min at 94°C; 39 cycles of 30 s at 94°C, 45 s at 60°C, and 2 min at 72°C; and 5 min at 72°C. Flanking sequences 5′ to the *dSpm* element were amplified with the following primer pairs: 5′-CCTGATTACGAGATGACAACACTG-3′ and 5′-GCACGACGGCTGTAGAATAGG-3′ (for Sau3AI) or 5′-CGCGCACCTCCAAGTAGC-3′ and 5′-GCACGACGGCTGTAGAATAGG-3′ (for RsaI). Sequences flanking the 3′ end of the *Spm* insertion were obtained with primer combinations 5′-ATTCATTCTGTTGGTGGGTCATTG-3′ and 5′-CTTAGAGTGTCGGCTTATTTCAGT-3′ (for Sau3AI) or 5′-GGACCGACGCTCTTATGTTAAAAG-3′ and 5′-CAGTAAGAGTGTGGGGTTTTGG-3′ (for RsaI). Gel-purified PCR products were subcloned into pCRII-TOPO (Invitrogen) for DNA sequencing. To identify the transcription start and polyadenylation site of *DRN/ESR1*, 5′ and 3′ rapid amplification of cDNA ends (RACE) experiments were performed as described (Comelli et al., 1999). Sequences of the *DRN/ESR1*-specific nested primers for 5′ RACE were 5′-AATTAGTACGAGCCTTTGC-3′ and 5′-GGTTTCTAGGGTTTT-

GGTTTG-3′; those for 3′ RACE were 5′-GTTCAAGAGACTAAGGAGAC-3′ and 5′-TCGCAGACGGTGGTTTATCG-3′. PCR products were subcloned into pCRII-TOPO (Invitrogen) and subjected to DNA sequence analysis.

Histological, Scanning Electron Microscopy, and GUS Analysis

Tissue for Dellafield staining was fixed overnight in 4% (w/v) paraformaldehyde in phosphate buffer, pH 7.0, and embedded in paraplast. After dewaxing with ROTIHISTOL (Roth, Karlsruhe, Germany), 7-μm sections were incubated for 2 to 3 min in Dellafield solution (Merck) and incubated in 0.5% (w/v) $NaHCO_3$ for color reaction. Detection of GUS activity and tissue preparation were performed as described (Sieburth and Meyerowitz, 1997), with minor modifications. GUS staining was performed for 5 h (*STM-GUS*), 90 min (*CLV3-GUS*), or 30 min (*DRN/ESR1-GUS*). For scanning electron microscopy, plant material was treated as described previously (Sommer et al., 1990).

Sequence Analysis

Sequence analyses were performed using the GCG Package, version 4.0 (Genetics Computer Group, Madison, WI). The PHYLIP program, version 3.6 (Felsenstein, 1986), was used to determine phylogenetic relationships.

Upon request, all novel materials described in this article will be made available in a timely manner for noncommercial research purposes.

ACKNOWLEDGMENTS

We thank Martin Hobe for initial help with the RNA in situ hybridizations, Lorenzo Borghi for scanning electron microscopy, Petra Comelli and Melanie Cole for excellent technical assistance, and John Chandler for critical reading of the manuscript. This work was supported by the Deutsche Forschungsgemeinschaft through We-1262/3-1, SFB 572, and Si 677/1-1. T.K. was funded by the Graduiertenkolleg "Molekulare Analyse von Entwicklungsprozessen" at the University of Cologne.

Received November 26, 2002; accepted December 23, 2002.

REFERENCES

Banno, H., Ikeda, Y., Niu, Q.W., and Chua, N.H. (2001). Overexpression of Arabidopsis ESR1 induces initiation of shoot regeneration. Plant Cell **13,** 2609–2618.

Bechtold, N., and Pelletier, G. (1998). In planta Agrobacterium-mediated transformation of adult *Arabidopsis thaliana* plants by vacuum infiltration. Methods Mol. Biol. **82,** 259–266.

Becker, D., Kemper, E., Schell, J., and Masterson, R. (1992). New plant binary vectors with selectable markers located proximal to the left T-DNA border. Plant Mol. Biol. **20,** 1195–1197.

Bowman, J.L., and Eshed, Y. (2000). Formation and maintenance of the shoot apical meristem. Trends Plant Sci. **5,** 110–115.

Bowman, J.L., Eshed, Y., and Baum, S.F. (2002). Establishment of polarity in angiosperm lateral organs. Trends Genet. **18,** 134–141.

Bradley, D., Carpenter, R., Sommer, H., Hartley, N., and Coen, E. (1993). Complementary floral homeotic phenotypes result from opposite orientations of a transposon at the plena locus of Antirrhinum. Cell **72,** 85–95.

Brand, U., Fletcher, J.C., Hobe, M., Meyerowitz, E.M., and Simon, R. (2000). Dependence of stem cell fate in *Arabidopsis* on a feedback loop regulated by CLV3 activity. Science **289,** 617–619.

Brand, U., Grünewald, M., Hobe, M., and Simon, R. (2002). Regulation of CLV3 expression by two homeobox genes in Arabidopsis. Plant Physiol. **129,** 565–575.

Brand, U., Hobe, M., and Simon, R. (2001). Functional domains in plant shoot meristems. Bioessays **23,** 134–141.

Chomczynski, P., and Sacchi, N. (1987). Single-step method of RNA isolation by acid guanidinium thiocyanate-phenol-chloroform extraction. Anal. Biochem. **162,** 156–159.

Comelli, P., König, J., and Werr, W. (1999). Alternative splicing of two leading exons partitions promoter activity between the coding regions of the maize homeobox gene *Zmhox1a* and *Trap* (transposon-associated protein). Plant Mol. Biol. **41,** 615–625.

Eckardt, N.A., Araki, T., Benning, C., Cubas, P., Goodrich, J., Jacobsen, S.E., Masson, P., Nambara, E., Simon, R., Somerville, S., and Wasteneys, G. (2001). Arabidopsis research 2001. Plant Cell **13,** 1973–1982.

Endrizzi, K., Moussian, B., Haecker, A., Levin, J.Z., and Laux, T. (1996). The *SHOOT MERISTEMLESS* gene is required for maintenance of undifferentiated cells in *Arabidopsis* shoot and floral meristems and acts at a different regulatory level than the meristem genes *WUSCHEL* and *ZWILLE*. Plant J. **10,** 967–980.

Eshed, Y., Baum, S.F., Perea, J.V., and Bowman, J.L. (2001). Establishment of polarity in lateral organs of plants. Curr. Biol. **11,** 1251–1260.

Felsenstein, J. (1986). Distance methods: A reply to Farris. Cladistics **2,** 130–144.

Fletcher, J.C., Brand, U., Running, M.P., Simon, R., and Meyerowitz, E.M. (1999). Signaling of cell fate decisions by CLAVATA3 in *Arabidopsis* shoot meristems. Science **283,** 1911–1914.

Jacqmard, A., Detry, N., Dewitte, W., Van Onckelen, H., and Bernier, G. (2002). In situ localisation of cytokinins in the shoot apical meristem of *Sinapis alba* at floral transition. Planta **214,** 970–973.

Lloyd, A.M., Schena, M., Walbot, V., and Davis, R.W. (1994). Epidermal cell fate determination in *Arabidopsis*: Patterns defined by a steroid-inducible regulator. Science **266,** 436–439.

Long, J.A., Moan, E.I., Medford, J.I., and Barton, M.K. (1996). A member of the KNOTTED class of homeodomain proteins encoded by the *STM* gene of *Arabidopsis*. Nature **379,** 66–69.

Lynn, K., Fernandez, A., Aida, M., Sedbrook, J., Tasaka, M., Masson, P., and Barton, M.K. (1999). The *PINHEAD/ZWILLE* gene acts pleiotropically in *Arabidopsis* development and has overlapping functions with the *ARGONAUTE1* gene. Development **126,** 469–481.

Mayer, K.F., Schoof, H., Haecker, A., Lenhard, M., Jürgens, G., and Laux, T. (1998). Role of *WUSCHEL* in regulating stem cell fate in the *Arabidopsis* shoot meristem. Cell **95,** 805–815.

McConnell, J.R., and Barton, M.K. (1998). Leaf polarity and meristem formation in Arabidopsis. Development **125,** 2935–2942.

McConnell, J.R., Emery, J., Eshed, Y., Bao, N., Bowman, J., and Barton, M.K. (2001). Role of PHABULOSA and PHAVOLUTA in determining radial patterning in shoots. Nature **411,** 709–713.

Murashige, T., and Skoog, F. (1962). A revised medium for rapid growth and bioassays with tobacco tissue culture. Physiol. Plant. **15**, 473–497.

Riechmann, J.L., and Meyerowitz, E.M. (1998). The AP2/EREBP family of plant transcription factors. Biol. Chem. **379,** 633–646.

Rupp, H.-M., Frank, M., Werner, T., Strnad, M., and Schmülling, T. (1999). Increased steady state mRNA levels of the *STM* and *KNAT1* homeobox genes in cytokinin overproducing *Arabidopsis thaliana* indicate a role for cytokinins in the shoot apical meristem. Plant J. **18,** 557–564.

Schneitz, K., Hülskamp, M., and Pruitt, R.E. (1995). Wild-type ovule development in *Arabidopsis thaliana*: A light microscope study of cleared whole-mount tissue. Plant J. **7,** 731–748.

Schoof, H., Lenhard, M., Haecker, A., Mayer, K.F., Jurgens, G., and Laux, T. (2000). The stem cell population of Arabidopsis shoot meristems is maintained by a regulatory loop between the CLAVATA and WUSCHEL genes. Cell **100,** 635–644.

Sieburth, L.E., and Meyerowitz, E.M. (1997). Molecular dissection of the *AGAMOUS* control region shows that cis elements for spatial regulation are located intragenically. Plant Cell **9,** 355–365.

Sommer, H., Beltran, J.P., Huijser, P., Pape, H., Lonnig, W.E., Saedler, H., and Schwarz-Sommer, Z. (1990). Deficiens, a homeotic gene involved in the control of flower morphogenesis in *Antirrhinum majus*: The protein shows homology to transcription factors. EMBO J. **9,** 605–613.

Tissier, A.F., Marillonnet, S., Klimyuk, V., Patel, K., Torres, M.A., Murphy, G., and Jones, J.D. (1999). Multiple independent defective suppressor-mutator transposon insertions in Arabidopsis: A tool for functional genomics. Plant Cell **11,** 1841–1852.

Überlacker, B., and Werr, W. (1996). Vectors with rare-cutter restriction enzyme sites for expression of open reading frames in transgenic plants. Mol. Breeding **2,** 293–295.

van der Graaff, E., Dulk-Ras, A.D., Hooykaas, P.J., and Keller, B. (2000). Activation tagging of the *LEAFY PETIOLE* gene affects leaf petiole development in *Arabidopsis thaliana*. Development **127,** 4971–4980.

Waites, R., Selvadurai, H.R., Oliver, I.R., and Hudson, A. (1998). The PHANTASTICA gene encodes a MYB transcription factor involved in growth and dorsoventrality of lateral organs in Antirrhinum. Cell **93,** 779–789.